

## A compact microscope for voltage imaging

Meng, Xin; Huismans, Lex; Huijben, Teun; Szabo, Greta; Van Tol, Ruud; De Heer, Izak; Ganapathy, Srividya; Brinks, Daan

**DOI**

[10.1088/2040-8986/ac5dd5](https://doi.org/10.1088/2040-8986/ac5dd5)

**Publication date**

2022

**Document Version**

Final published version

**Published in**

Journal of Optics (United Kingdom)

**Citation (APA)**

Meng, X., Huismans, L., Huijben, T., Szabo, G., Van Tol, R., De Heer, I., Ganapathy, S., & Brinks, D. (2022). A compact microscope for voltage imaging. *Journal of Optics (United Kingdom)*, 24(5), Article 054004. <https://doi.org/10.1088/2040-8986/ac5dd5>

**Important note**

To cite this publication, please use the final published version (if applicable).  
Please check the document version above.

**Copyright**

Other than for strictly personal use, it is not permitted to download, forward or distribute the text or part of it, without the consent of the author(s) and/or copyright holder(s), unless the work is under an open content license such as Creative Commons.

**Takedown policy**

Please contact us and provide details if you believe this document breaches copyrights.  
We will remove access to the work immediately and investigate your claim.

PAPER • OPEN ACCESS

## A compact microscope for voltage imaging

To cite this article: Xin Meng *et al* 2022 *J. Opt.* **24** 054004

View the [article online](#) for updates and enhancements.

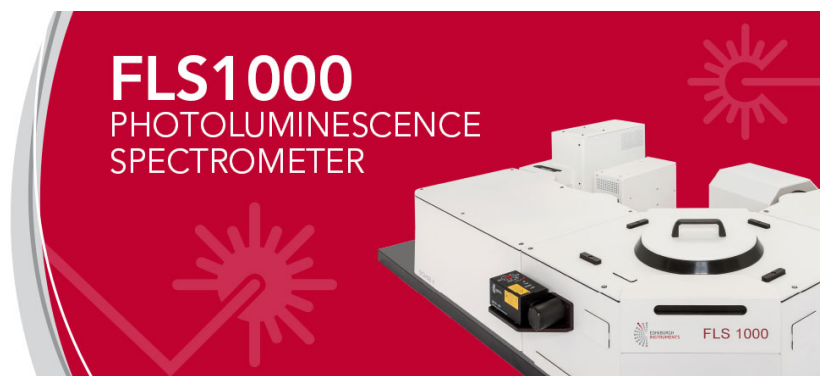
You may also like

- [Towards the development of new generation spin-orbit photonic techniques](#)  
Athira B S, Mandira Pal, Sounak Mukherjee *et al.*
- [Multi-value phase grating fabrication using direct laser writing for generating a two-dimensional focal spot array](#)  
Yi Huang, Minglong Li, Pu Tu *et al.*
- [Recent advances on strong light-matter coupling in atomically thin TMDC semiconductor materials](#)  
Ibrahim A M Al-Ani, Khalil As'ham, Oleh Klochan *et al.*



**EXPERTS IN  
FLUORESCENCE.**

edinst.com



# A compact microscope for voltage imaging

Xin Meng<sup>1</sup> , Lex Huismans<sup>1</sup>, Teun Huijben<sup>1,3</sup> , Greta Szabo<sup>1,3</sup>, Ruud van Tol<sup>1</sup>, Izak de Heer<sup>1</sup>, Srividya Ganapathy<sup>1</sup> and Daan Brinks<sup>1,2,\*</sup> 

<sup>1</sup> Department of Imaging Physics, Delft University of Technology, Delft, The Netherlands

<sup>2</sup> Department of Molecular Genetics, Erasmus University Medical Center, Rotterdam, The Netherlands

E-mail: [d.brinks@tudelft.nl](mailto:d.brinks@tudelft.nl)

Received 12 January 2022, revised 23 February 2022

Accepted for publication 15 March 2022

Published 1 April 2022



## Abstract

Voltage imaging and optogenetics offer new routes to optically detect and influence neural dynamics. Optimized hardware is necessary to make the most of these new techniques. Here we present the Octoscope, a versatile, multimodal device for all-optical electrophysiology. We illustrate its concept and design and demonstrate its capability to perform both 1-photon and 2-photon voltage imaging with spatial and temporal light patterning, in both inverted and upright configurations, *in vitro* and *in vivo*.

Supplementary material for this article is available [online](#)

Keywords: electrophysiology, neuroscience, microscopy

(Some figures may appear in colour only in the online journal)

## 1. Introduction

Voltage imaging is a novel technique to probe neural dynamics, allowing the visualization of cellular electrical dynamics through transduction of changes in cell membrane voltage into changes in fluorescence of a molecular probe embedded in the cell membrane. These probes can either be small molecules [1] or engineered proteins called genetically encoded voltage indicators (GEVIs) [2, 3]. Voltage imaging can be combined with optogenetic actuators: light-sensitive ion channels or pumps that, upon expression in cells, allow illumination based control of cellular electrical activity [4–6]. The combination is referred to as all-optical electrophysiology [7].

While GEVI and voltage imaging assay development have sometimes been done on commercial microscope scaffolds [1, 8, 9], custom-built apparatus has often been deemed necessary to achieve optimal results [7, 10–13]. The potential of all-optical electrophysiology to contribute to the answering of neuroscientific questions relies on the availability of microscopes that make optimal use of the advantages voltage imaging offers: recording voltage dynamics at high temporal resolution (<1 ms), over a large number of cells, in 2D and 3D cellular environments and with the flexibility to accommodate different types of samples and experiments. Patterned illumination is often a necessary strategy for signal-to-background discrimination in voltage imaging [12, 13] or cellular stimulation in all-optical electrophysiology [7]. These needs are intensified by the fact that the protein sensors used in voltage imaging have interesting photophysical properties. For example, voltage sensitivity of sensors can change depending on the illumination scheme [14]; and dynamics can occur that allow accessing different states in the photocycle depending on the coincidence of light absorption events and voltage changes [15]. Combined optical and molecular development leads to novel measurement modalities [12–14, 16–18] that

<sup>3</sup> These authors contributed equally to this work.

\* Author to whom any correspondence should be addressed.



Original content from this work may be used under the terms of the [Creative Commons Attribution 4.0 licence](#). Any further distribution of this work must maintain attribution to the author(s) and the title of the work, journal citation and DOI.

ideally can be developed on the same setup where they are to be applied as in vivo neuroscientific assays.

Many voltage imaging applications use one-photon (1P) imaging for both GEVI development and voltage imaging assays [19–21], though recent years has seen the advent of two-photon (2P) voltage imaging [14, 22]. Thus, a microscope that has the above flexibility in both 1P and 2P imaging modalities would be an ideal platform for optimization and application of voltage imaging and all-optical electrophysiological assays. Here we introduce the Octoscope, a compact design for a microscope that features imaging and patterned illumination with 1P or 2P illumination and recording on a widefield camera or photomultiplier tube (PMT). Crucially, the design and its compactness allow a precise and reproducible orientation of the objective throughout a 360° angle of rotation, allowing voltage imaging, patterned illumination, optogenetics and all-optical electrophysiology experiments in upright and inverted configurations and at custom angles of the objective. Although microscopes combining 1P and 2P excitation [23], microscopes that are able to pattern illumination [24] and microscopes that switch between upright and inverted configurations exist [25], to our knowledge none of them combine all these features, let alone in a compact and automated package.

## 2. Method

### 2.1. Octoscope concept and custom designs

The Octoscope consists of two illumination pathways, two detection pathways and currently two imaging configurations (upright and inverted) for a total of eight different optical stimulation and imaging modalities. This flexibility is made possible by a custom designed beam combiner (figure 1(a)) and objective holder, featuring exchangeable dichroic mirrors and filters and motorized objective translation and rotation. (figure 1(b)).

This holder is embedded in a setup featuring a 2P illumination pathway through scanning galvanometric mirrors (6215HR, Cambridge Technology), a 1P illumination pathway via a Digital Micromirror Device (DMD, Vialux V7001, Texas Instruments), and detection on a camera or a PMT pathway with motorized switching between the two (figure 1(c)). The beam combiner and objective holder, made of anodized aluminum, mounts the tube lenses for 1P excitation, 2P excitation and the detection pathways. The configuration used in the experiments in this paper employs 200 mm tube lenses (TTL200, Thorlabs). The beam combiner and objective holder contains exchangeable holders for the dichroic mirrors that combine the 1P and 2P excitation pathway and separate excitation and emission pathways (figure 1(d)). The objective is mounted on a translation stage (M110-DG, Physik Instrumente) which drives linear translation of the objective for focus adjustment. This translatable objective holder contains a prism reflector mounted on the rotation axis of a rotation motor (RS-40, Physik Instrumente) to allow rotation of the objective.

Scan head and scan lens of the 2P excitation pathway are mounted in a custom aluminum holder (figure 1(e)). The scanning module is fixed on a large-area translation stage

(TBB1515/M, Thorlabs) so that the scanning mirrors and the scan lens can move along the optical axis for fine adjustment of the focal plane. A compact lens mount with reflection mirror on the holder turns the incident laser beam 90° and directs it to the first scanning mirror, allowing adjustment of the scanning module position without changes in alignment of the excitation beam. The scan lens is fixed to the block in a 3D printed V-clamp.

### 2.2. 1P excitation pathway

In our lab, 1P illumination was provided by three continuous wave lasers (MLL-III-532, CNI; MLL-FN-639, CNI; OBIS 488 LX, Coherent). Their output is made uniform in polarization and beam diameter through zero-order half-wave plates (WPH05M-488, WPH05M-532, WPH05M-633, Thorlabs) and polarizers (CCM5-PBS201/M, Thorlabs) and individual collimators (AC254 mounted achromatic doublets, Thorlabs). The laser beams are then combined using dichroic mirrors (DMLP505, DMLP605, Thorlabs) and lead through an acousto-optic tunable filter (AOTFnc-VI S; AA Optoelectronics) with a modulation rate of 22 kHz to allow fast intensity modulation. Beam diameter is adjusted with a variable telescope (AC254 mounted achromatic doublets, Thorlabs) using flip mounts (TRF90/M, Thorlabs). The beam is guided into the setup over the DMD to allow patterned illumination of the sample. A dichroic mirror (Di03-R405/488/532/635-t3-32 × 44, Semrock) mounted in the dichroic holder of the beam combiner separates the excitation lines from the fluorescence emission.

### 2.3. 2P excitation pathway

We employ 2P excitation using a Spectra-Physics InSight X3 with a tunable range from 680 to 1300 nm, 120 fs pulse width and an average power of 1.4 W at 1200 nm. A high speed laser shutter (LS2, Uniblitz) is used for binary modulation of the laser beam. Neutra Density (ND) filters are used for analog modulation of the laser beam intensity. The beam is then magnified by a telescope (AC254-150-B-ML and AC254-500-B-ML, Thorlabs) to 5 mm in diameter, and guided to the galvanometric mirrors. The same input port can be used as a separate 1P excitation pathway for widefield illumination without spatial patterning.

To project the beam to the back aperture of the objective, a scan lens (SL50-2P2, 50 mm focal length, Thorlabs) is combined with the octoscope tube lens (TTL200MP, Thorlabs) to gain a total magnification factor of 4. The resulting maximum diffraction limited field of view (FOV) is determined by the scan lens in the scanning system, 14.1 × 14.1 mm after the scan lens at the intermediate plane. A long-pass dichroic mirror (Di03-R785-t3-32 × 44, Semrock) passes the 2P excitation beam into the objective and reflects the 1P excitation and fluorescence emission.

### 2.4. Emission pathways

Emitted fluorescence is collected by the objective, focused by the imaging tube lens (TTL200, 200 mm focal length,

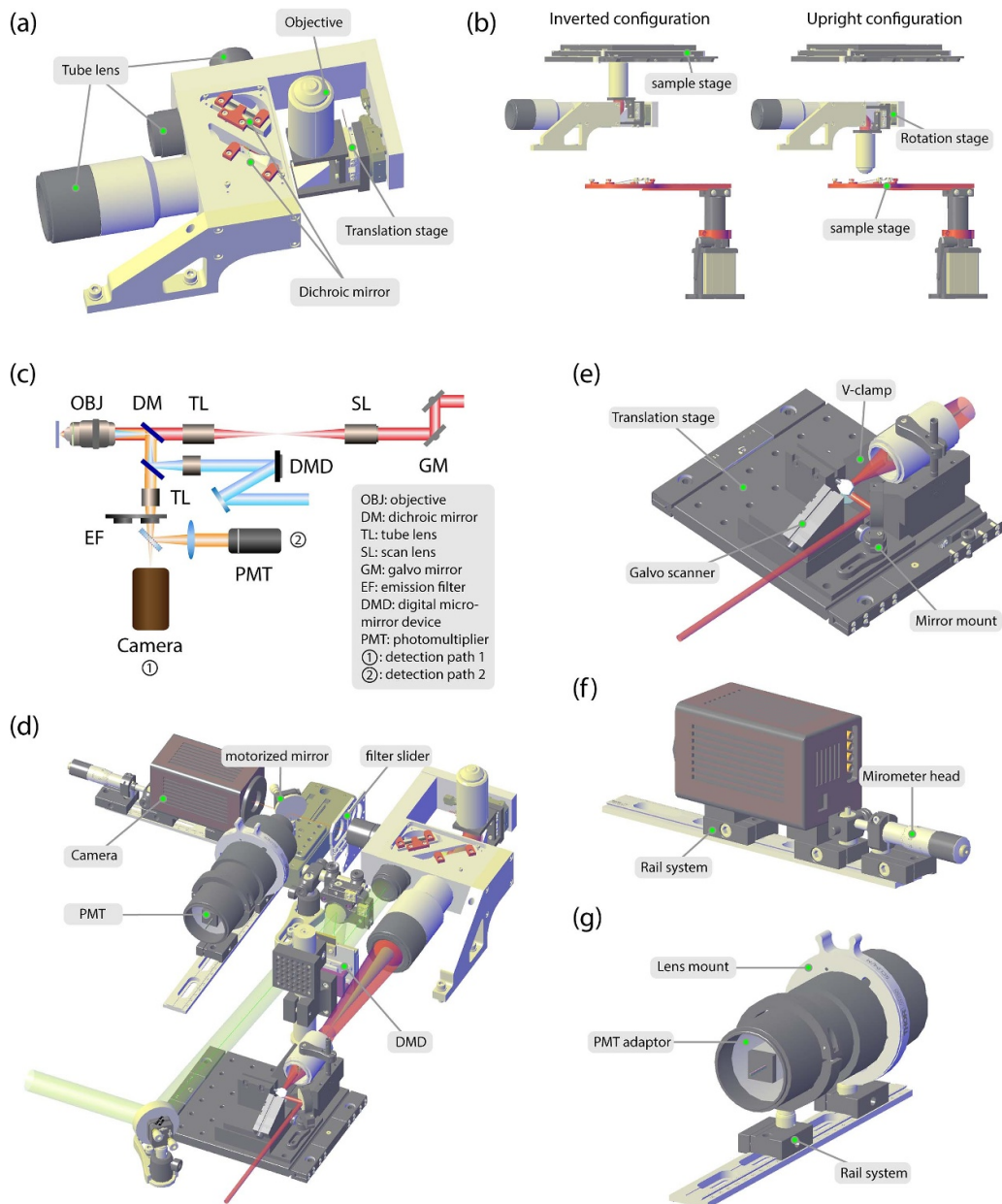


**Figure 1.** Octoscope design. (a) The customized beam combiner block. (b) The beam combiner and objective holder allow automated switching between upright and inverted configurations. (c) Schematic of the 1P and 2P excitation pathways, combined and separated from the emission pathways; (d) the beam combiner and objective holder allows combination of a 1P and 2P excitation pathway with camera and PMT detection. (e) Mount for the 2P scan head. (f) Camera translation system. (g) PMT mount.

Thorlabs), and then filtered by emission filters placed in a linear translation mount (ELL9, Thorlabs). In the experiments described in this paper, these are band-pass filters (FF01-560/94-25, FF01-582/64-25, LP02-664RU-25 and FF01-790/SP-25, SemRock). The signal is then passed to detection pathway one, or redirected by a mirror mounted on a motorized translation stage (DDSM50/M, Thorlabs) to detection pathway two. In our lab, we positioned a sCMOS camera (ORCA Flash4.0 V3, Hamamatsu; 2048 × 2048 pixels, 6.5 μm pixel size) on a rail system (XT34HP/M, Thorlabs) with 3D printed adapter and a micrometer head (150–801ME, Thorlabs) for fine adjustment of the focal position in detection pathway one (figure 1(f)). In this pathway, the recording speed

reaches 500 Hz over a 95 μm × 477 μm FOV and 1000 Hz at 48 μm × 477 μm FOV. In pathway two, we used an aspherical lens (LAGC065, Ross Optical) to project the back aperture of the objective onto a PMT. We mounted PMTs (H10721-01, peak sensitivity at 400 nm; H10721-20, peak sensitivity wavelength at 630 nm; Hamamatsu) in a custom 3D printed adaptor for easy mounting and switching (figure 1(g)) in a Thorlabs SM2 lens tube.

In the described configuration, beam combiner, objective holder and tube lens holder are all part of a micro-machined whole, which makes the compact geometry of the octoscope possible; nevertheless, the objective focal plane, 2P excitation plane and camera image plane can all be independently aligned

for perfect overlap with the sample plane using the described custom translation mounts.

### 2.5. Electrophysiology setup

While not a defining feature of the octoscope, we describe here the electrophysiology modules used for the experiments described in this paper. We use a motorized stage for petri dish positioning in the inverted configuration (BioPrecision2, Ludl), and a homebuilt sample holder in the upright configuration. In our lab, we added a patch clamp amplifier (Model 2400, A-M Systems) and a micromanipulator (Patch-Star system, Scientifica) for patch clamp electrophysiology, which enables fast, faithful recording and control of current through and voltage across the cell membrane, which provides a ground truth measurement for the membrane voltage or current dynamics of an individual cell [26]. We supplemented this with a perfusion system (TC-1-100, TC-E50  $\times$  30, TC-1-100S, PS-8H, Bioscience tools).

### 2.6. Synchronization and software

Device triggering, control signals for the Galvanometric mirrors, AOTF and patch clamp electronics, and detection of signals from the patch clamp amplifier are provided by coupled Input/output devices (USB-6363, National Instruments). The output current from the PMT is amplified by a trans-impedance amplifier (DHPCA-100, FEMTO), and filtered by a programmable electronic filter (USBPGF-S1, Alligator technologies) before being sampled. The camera uses a Camera Link card (FireBird PCI Express Gen II 8 $\times$ ) for data acquisition.

Dedicated instrument control software was written in Python, with hardware control interface backend and user interface frontend. (<https://github.com/Brinkslab/Octoscope.git>)

## 3. Results and discussion

### 3.1. Imaging specifications

In the experiments described here, a long working distance multiphoton microscopy objective is used (Olympus XLPLN25XWMP2, NA 1.05, working distance 2 mm), for a total magnification of the imaging system of 27.8. Calibration of the FOV provides, in combination with the used excitation and emission pathways, a  $507 \times 507 \mu\text{m}$  FOV for 2P imaging and a diffraction limited resolution of  $\sim 500 \text{ nm}$  at 1200 nm excitation; and a  $490 \times 490 \mu\text{m}$  FOV for 1P imaging with an image pixel size of 233 nm (based on the employed camera).

### 3.2. Multimodal imaging

Fluorescence imaging under widefield 1P excitation (figure 2(a)) provides spatial (figure 2(b)) and temporal (figure 2(c), supplementary video 1 available online at

[stacks.iop.org/JOpt/24/054004/mmedia](https://stacks.iop.org/JOpt/24/054004/mmedia)) information at resolutions suitable for voltage imaging. For higher time resolution recordings, the PMT can be used for data acquisition (figure 2(d)). In the widefield pathway, patterned illumination using the DMD can be used to specifically illuminate parts of the sample of interest to record e.g. voltage responses of GEVIs with microsecond accuracy (figure 2(e)). Similarly, 2P excitation of the sample and collection of fluorescence on the PMT (figure 2(f)) can be employed for standard raster scanning imaging (figure 2(g)) or patterned illumination where the membrane of a cell can be traced for selective excitation of fluorescence and recording with high time resolution (figure 2(h)). Strong photo bleaching is seen in the shown measurement because of the high excitation power used (90 mW after objective). 2P excitation can also be employed with image projection on the camera (figures 2(i) and (j), supplementary video 2) for e.g. laser etching [27], local ablation [28] or optogenetic stimulation [29] combined with sample inspection or voltage imaging.

### 3.3. Objective orientation

The rotational motor grants the setup the ability to easily convert between upright and inverted configurations. (figure 3(a)) and effortlessly perform imaging and patterned illumination in both (figure 3(b)). The needed time to convert the configurations only depends on the motor rotating speed, which is currently set to 45 s in our setup (figure 3(c), supplementary video 3). In this demonstration experiment, two zebrafish larvae expressing GCaMP6s were positioned onto the two sample stages associated with the inverted and upright configurations. Widefield images of both fish were recorded after which two DMD illumination patterns were created, one for the top fish and one for the bottom fish. The measurements demonstrate automated reproducible positioning of the objective and parallel automated switching of illumination patterns, as both fish are illuminated with their appropriate cell selecting DMD patterns. The multimodal capabilities of the octoscope make it, in the context of voltage imaging, suitable for a range of optogenetic and all-optical electrophysiology experiments, ranging from recordings of protein dynamics [16], single cell and sub-cellular voltage dynamics [13] to *in vivo* imaging in behavioral assays [12].

### 3.4. Large scale screening imaging

The microscope is able to perform large scale imaging by automated tiling of acquired FOVs with both 1P and 2P excitation. Figure 4(a) shows the image from a single FOV acquisition with 2P excitation, tuned to  $340 \mu\text{m} \times 340 \mu\text{m}$  of sample of cultured HEK293T cells expressing QuasAr1. A zoom-in inspection is shown in figure 4(b), with a pixel resolution of 680 nm. To sample over cells across the petri-dish,  $18 \times 18$  FOVs were automatically imaged and stitched (figure 4(c)). The total area is  $6.12 \times 6.12 \text{ mm}$ , with the diagonal being 8.45 mm. This type of large scale tiled imaging is useful for e.g. screens of protein or drug libraries.

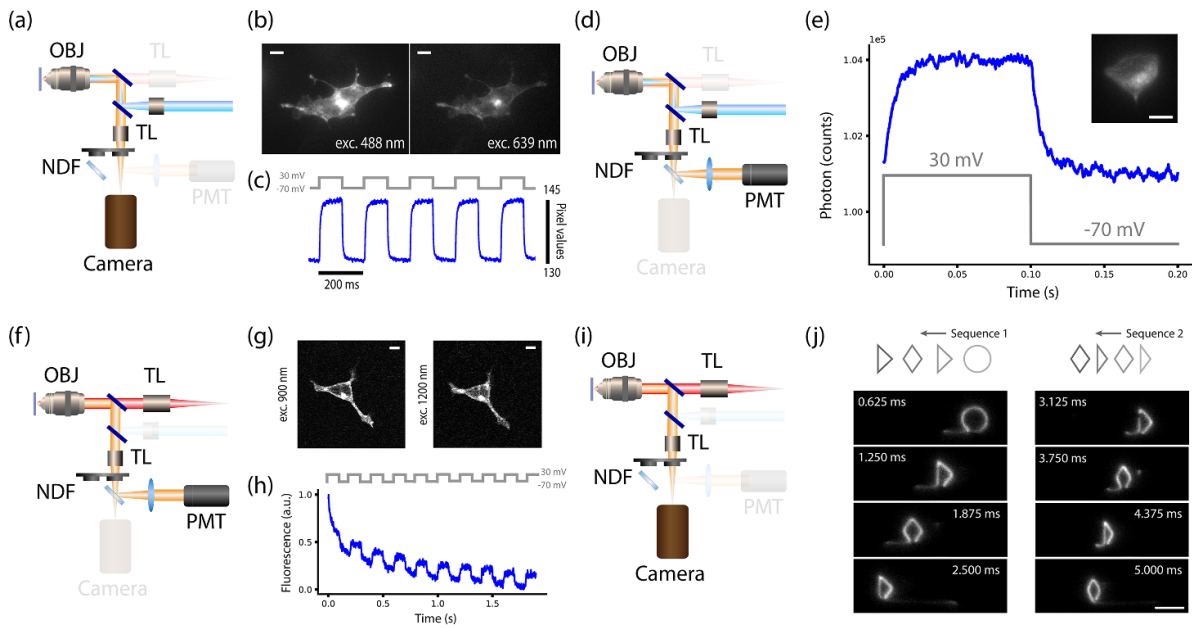


**Figure 2.** Four types of measurements using four different octoscope configurations. (a) Schematic diagram of camera imaging under 1P excitation. (b) Human embryonic kidney 293T cells (HEK293T cells) expressing Archon1-eGFP [10] under 488 nm excitation (left) and 639 nm excitation (right). (c) Fluorescence trace from camera recording of HEK293T cell expressing Archon1 imaged at 639 nm while membrane potential is changed in steps. (d) Schematic of PMT imaging under 1P excitation. (e) Fluorescence recording of a HEK293T cell expressing Archon1 upon altering its membrane potential with a time resolution of 50  $\mu$ s. (f) Schematic diagram of PMT recording under 2P excitation. (g) 2P image of a HEK293T cell expressing QuasAr1-Citrine [7] under excitation of 900 nm (left) and 1200 nm (right) wavelength. (h) Fluorescence trace from PMT recording under 2P contour scan conditions. (i) Schematic diagram of camera imaging under 2P excitation. (j) Camera recording under 2P patterning (supplementary video 2). Switching laser patterns written into the sample at a switching rate of 1.6 kHz. All scale bars: 10  $\mu$ m.

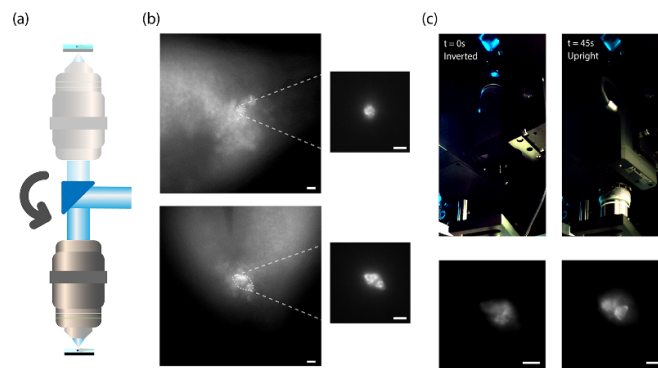


**Figure 3.** Automated inversion of microscope orientation. (a) Sketch of the switching principle. (b) Zebrafish larvae expressing GCaMP6s imaged under widefield excitation with 488 nm, and under DMD projection upon selected cells in dashed line (insert). (c) Two zebrafish larvae expressing GCaMP6s imaged sequentially in inverted (left) and upright configuration (right) in a single automated experiment. Scalebars: 10  $\mu$ m.

### 3.5. Patterned illumination

Shaping the illumination reduces background fluorescence and improves the signal to noise ratio tremendously, especially for *in vivo* imaging. The Octoscope is able to pattern both 1P and 2P excitation light onto selected regions with sufficient accuracy to not only tag the cell body (figure 5(a), left), but also the cell membrane (figure 5(a), right). This is useful for voltage imaging as the voltage sensitive fluorescence is collected from GEVIs located in the cell membrane, and therefore only the outer edge of the cell provides useful signal, as opposed to for

instance calcium imaging where useful signal can be recorded from the entire cytosol. The cells marked with white dotted lines were selected for projection. The bottom left figure shows whole cell patterning, while the bottom right figure only has the cells' membrane projected. This patterning is also possible *in vivo*. Figure 5(b) top left displays a widefield image of a zebrafish larva expressing GCaMP6s, flood illuminated with 488 nm. Fluorescence from different depth contributes to background fluorescence and noise. Patterned illumination was applied to the cell membrane (in dashed square) using

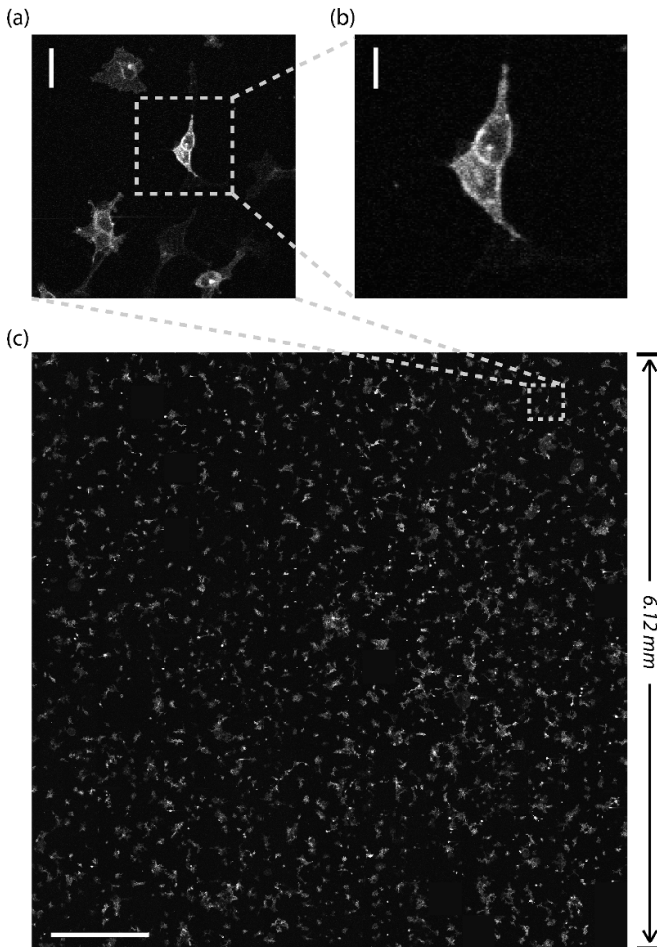


**Figure 4.** Large scale screening 2P imaging under 1200 nm excitation. (a) Single FOV image of a cell culture of HEK293T cells expressing Archon1. Scale bar: 50  $\mu\text{m}$ . (b) Digital zoom only shows sufficient resolution to mark the cell membrane. Scale bar: 20  $\mu\text{m}$ . (c) Large scale image of the same sample with an 8.45 mm diagonal. Scale bar: 1 mm. All images taken on the octoscope.

the DMD and 1P excitation (figure 5(b), top right) and using the galvo scanners and 2P excitation (figure 5(c), top right). Cross section profiles of the cell fluorescence (dashed horizontal lines in figures 5(b) and (c) bottom), show accurate patterning of the cell membrane in both modalities and a marked increase in SNR and decrease in background fluorescence for both 1P and 2P patterned illumination.

Patterned illumination with 2P excitation could benefit from several upgrades to the setup: z-axis scan speed can be improved by incorporation of a remote focus unit or a deformable lens; acousto-optical deflectors could be used for an improvement in speed in sequential patterning; or spatial light modulators in combination with temporal focusing could be used for parallel 2P patterning in three dimensions. All of these improvements would increase the time resolution of 3D patterning, but would have to be carefully considered in terms of tradeoffs regarding either compactness of the microscope (if new pathways are added to house the upgrades) or achievable FOV, throughput and resolution.

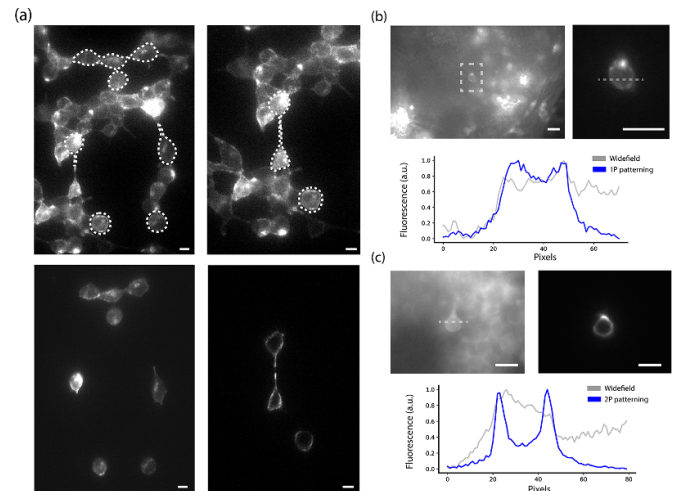


**Figure 5.** Patterned illumination on the octoscope can mark cell bodies and cell membranes *in vitro* and *in vivo*. (a) HEK293T cell cultures (top) imaged with 488 nm excitation. DMD patterning of cell bodies (bottom left) and cell membranes (bottom right) is possible. (b) Top left: widefield image of cells expressing GCaMP6s in zebrafish larva, excited at 488 nm. Top right: 1P patterning of 488 nm illumination on cell membrane. Bottom: cross section along the dotted line in widefield and patterned illumination mode. (c) Top left: widefield image of cells in zebrafish larva under 488 nm excitation. Top right: 2P patterning of 900 nm illumination on the chosen cell membrane. Bottom: cross section along the dotted line in 1P widefield and 2P patterned illumination mode. Scale bars: 10  $\mu\text{m}$ .

## 4. Conclusion

We demonstrate a compact, versatile, multimodal microscope with patterned illumination capabilities and the temporal and spatial resolution necessary for voltage imaging in 1P and 2P excitation schemes, in inverted and upright configurations. The compact design and hardware automation make advanced physical and biological imaging experiments in physical and biological samples possible on the same setup without the need for elaborate hardware reconfigurations or realignment. Patterned illumination capabilities at high spatial and temporal resolution allow a spectrum of voltage imaging, optogenetic and all-optical electrophysiological experiments, of which we have shown a few proof-of-principle examples.

## Data availability statement

All data that support the findings of this study are included within the article (and any supplementary files).




## Acknowledgments

We thank Adam Cohen for the gift of QuasAr1 (derived from Addgene plasmid # 59172), Ed Boyden for the gift of Archon1 (Addgene plasmid # 108423), and Elizabeth Carroll, Laura Maddalena and Zhenzhen Wu for use of zebrafish larvae. DB acknowledges support by an NWO Start-up



Grant (740.018.018) and ERC Starting Grant (850818—MULTIVision).

## ORCID iDs

Xin Meng  <https://orcid.org/0000-0002-7071-2842>  
 Teun Huijben  <https://orcid.org/0000-0002-8984-2882>  
 Daan Brinks  <https://orcid.org/0000-0002-5550-5140>

## References

- [1] Miller E W 2016 Small molecule fluorescent voltage indicators for studying membrane potential *Curr. Opin. Chem. Biol.* **33** 74–80
- [2] Yang H H and St-Pierre F 2016 Genetically encoded voltage indicators: opportunities and challenges *J. Neurosci.* **36** 9977
- [3] Xu Y, Zou P and Cohen A E 2017 Voltage imaging with genetically encoded indicators *Curr. Opin. Chem. Biol.* **39** 1–10
- [4] Nagel G, Szellas T, Huhn W, Kateriya S, Adeishvili N, Berthold P, Ollig D, Hegemann P and Bamberg E 2003 Channelrhodopsin-2, a directly light-gated cation-selective membrane channel *Proc. Natl Acad. Sci.* **100** 13940–5
- [5] Zhang F, Wang L-P, Boyden E S and Deisseroth K 2006 Channelrhodopsin-2 and optical control of excitable cells *Nat. Methods* **3** 785–92
- [6] Gradmann D, Berndt A, Schneider F and Hegemann P 2011 Rectification of the channelrhodopsin early conductance *Biophys. J.* **101** 1057
- [7] Hochbaum D R et al 2014 All-optical electrophysiology in mammalian neurons using engineered microbial rhodopsins *Nat. Methods* **11** 825–33
- [8] Yang H H, St-Pierre F, Sun X, Ding X, Lin M Z and Clandinin T R 2016 Subcellular imaging of voltage and calcium signals reveals neural processing in vivo illuminates neuronal computations *in vivo*, including the origin of ON and OFF selectivity *Cell* **166** 245–57
- [9] Piatkevich K D et al 2019 Population imaging of neural activity in awake behaving mice *Nature* **574** 413–7
- [10] Piatkevich K D et al 2018 A robotic multidimensional directed evolution approach applied to fluorescent voltage reporters article *Nat. Chem. Biol.* **14** 352–60
- [11] Werley C A, Chien M-P and Cohen A E 2017 Ultrawidefield microscope for high-speed fluorescence imaging and targeted optogenetic stimulation *Biomed. Opt. Express* **8** 5794–813
- [12] Adam Y et al 2019 Voltage imaging and optogenetics reveal behaviour-dependent changes in hippocampal dynamics *Nature* **569** 413–7
- [13] Chien M-P, Brinks D, Testa-Silva G, Tian H, Phil Brooks F, Adam Y, Bloxham W, Gmeiner B, Kheifets S and Cohen A E 2021 Photoactivated voltage imaging in tissue with an archaerhodopsin-derived reporter *Sci. Adv.* **7** abe3216
- [14] Brinks D, Klein A J and Cohen A E 2015 Two-photon lifetime imaging of voltage indicating proteins as a probe of absolute membrane voltage *Biophys. J.* **109** 914–21
- [15] Penzkofer A, Silapetere A and Hegemann P 2021 Photocycle dynamics of the Archaerhodopsin 3 based fluorescent voltage sensor Archon2 *J. Photochem. Photobiol. B* **225** 112331
- [16] Venkatachalam V, Brinks D, Maclaurin D, Hochbaum D, Kralj J and Cohen A E 2014 Flash memory: photochemical imprinting of neuronal action potentials onto a microbial rhodopsin *J. Am. Chem. Soc.* **136** 2529–37
- [17] Venkatachalam V and Cohen A E 2014 Imaging GFP-based reporters in neurons with multiwavelength optogenetic control *Biophys. J.* **107** 1554–63
- [18] Tian H et al 2021 All-optical electrophysiology with improved genetically encoded voltage indicators reveals interneuron network dynamics *in vivo bioRxiv* p 2021.11.22.469481 (November)
- [19] Ataka K and Pieribone V A 2002 A genetically targetable fluorescent probe of channel gating with rapid kinetics *Biophys. J.* **82** 509–16
- [20] Han Z, Jin L, Platasa J, Cohen L B, Baker B J and Pieribone V A 2013 Fluorescent protein voltage probes derived from arlight that respond to membrane voltage changes with fast kinetics *PLoS One* **8** e81295
- [21] St-Pierre F, Marshall J D, Yang Y, Gong Y, Schnitzer M J and Lin M Z 2014 High-fidelity optical reporting of neuronal electrical activity with an ultrafast fluorescent voltage sensor *Nat. Neurosci.* **17** 884–9
- [22] Li B, Chavarha M, Kobayashi Y, Yoshinaga S, Nakajima K, Lin M Z and Inoue T 2020 Two-photon voltage imaging of spontaneous activity from multiple neurons reveals network activity in brain tissue *iScience* **23** 101363
- [23] Andrasfalvy B K, Zemelman B V, Tang J and Vaziri A 2010 Two-photon single-cell optogenetic control of neuronal activity by sculpted light *Proc. Natl Acad. Sci. USA* **107** 11981–6
- [24] Fan L Z et al 2020 All-optical electrophysiology reveals the role of lateral inhibition in sensory processing in cortical layer 1 *Cell* **180** 521–35.e18
- [25] Mayrhofer J M et al 2015 Design and performance of an ultra-flexible two-photon microscope for *in vivo* research *Biomed. Opt. Express* **6** 4228
- [26] Neher E and Sakmann B 1992 The patch clamp technique *Sci. Am.* **266** 44–51
- [27] Ouyang H, Deng Y, Knox W H and Fauchet P M 2007 Photochemical etching of silicon by two photon absorption *Phys. Status Solidi* **204** 1255–9
- [28] Liang X, Michael M and Gomez G A 2016 Measurement of mechanical tension at cell-cell junctions using two-photon laser ablation *Bio-protocol* **6** e2068
- [29] Prakash R et al 2012 Two-photon optogenetic toolbox for fast inhibition, excitation and bistable modulation *Nat. Methods* **9** 1171–9